Hybrid heat pump demand response potential estimation in UK households using physics-informed machine learning

Shuwen Liu[a], Olly Smith[a], David Shipworth[a]

[a]Energy Institute, University College London, Gower Street, London, WC1E 6BT, United Kingdom

Abstract

Hybrid heat pumps (HHPs) have arisen as a pragmatic variant of heat pumps for domestic space and hot water heating. As a heating device that combines a gas boiler and an air-source heat pump, HHPs can electrify a significant amount of the domestic heat demand, without requiring thermal upgrade or storage. One of the most important features of HHPs is flexibility provision, i.e., providing demand response by leveraging building thermal mass and switching between fuels. There has been limited large-scale field trial data of HHP flexibility in the UK, and few studies that realistically represent the short-run thermal dynamics of buildings. This study addresses this gap in the modelling by constructing a machine learning model based on the Lumped Capacitance Model to represent domestic building thermal dynamics, extracting information from monitoring data from over 700 UK dwellings. Optimized heating operation is then simulated to estimate the potential for demand response within thermally acceptable bounds under a tariff-based flexibility mechanism. The impact of building thermal properties and the tariff structure on HHP demand response potential is examined. It is found that even during peak wintertime, HHPs with an output capacity of 4kW can electrify 86% percent of the heating demand, while providing 77% of monovalent heat pump (MHP) peak time demand response in addition to reduced baseline peak demand, without compromising on thermal comfort. This study constructs a portfolio of empirically grounded building energy flexibility models, which can be easily integrated into a distribution-level power network model, to investigate the impact of HHP domestic heating flexibility in a wider system.

Keywords: Hybrid Heat Pumps; Energy Flexibility; Demand Response; Grey-Box Modeling; Lumped Capacitance Model

1. Introduction

1.1. Background

Space and water heating accounts for 23% of UK Green House Gas emissions, 17% from homes [1]. Decarbonizing heating is therefore critical to meeting legislated government targets. Electric heat pumps are central to UK government ambitions, which target 600,000 annual installations by 2028 [2]. However, large-scale deployment of electrical heat pumps faces challenges: grid overloading, high upfront and operating costs, efficiency losses in cold weather, and substantial heating system replacement [3], [4], [5],[6],[7],[8].

Hybrid heat pumps (HHP), combining an air-to-water heat pump with a gas boiler, offer an alternative solution [9]. They reduce upfront cost by using existing boilers for peaks and hot water, enabling smaller heat pump units, avoiding hot water cylinders, and minimizing retrofit needs [10], [11], [12]. This lowers installation disruption and may accelerate deployment by easing short-term supply-chain pressure. Boilers also generate backup heat during cold spells when heat pump COPs fall. Depending on the long-term evolution of the energy system, HHPs can either serve temporarily or indefinitely, in a future where electricity and zero-carbon gas coexist.

HHPs are designed to operate flexibly. The UK's 2030 Clean Power Plan relies on intermittent renewables [13] while electrified heating and transport may double or triple aggregated residential electricity demand [5], [14], [15], necessitating significant network reinforcement. Demand-side flexibility is essential for coping with the above challenges. In this context, the system impacts of HHPs and monovalent heat pumps (MHPs) need to be compared to guide the deployment of both technologies.

Based on Li et al. [16], "demand-side energy flexibility"(hereinafter "flexibility") refers to the ability to adjust electricity demand (and storage/generation, if applicable) to support power network requirements. A related concept, "demand response," describes changes in electricity usage activated to support network operation. Residential flexibility can be activated via direct control, voluntary turn-up/turn-down, or time-varying tariffs. HHPs provide flexibility in two ways:

- Fuel switching: shifting heat provision between electricity and gas.
- Load shifting: using thermal storage (in the building fabric, or domestic hot-water tank, which is normally unnecessary for HHPs) to move heating and thus electricity demand to periods of lower system stress.

Relative to MHPs, HHPs can provide flexibility over longer timeframes, particularly during extended 'dunkelflaute' events when renewable generation is low. At the power system level, this flexibility may:

- Reduce peak demand and mitigate reinforcement needs in electrical distribution and transmission networks.
- Provide balancing services across timescales, from fast frequency response to longer-term reserve, to reduce curtailment of intermittent renewables and replace dispatchable generation and storage. [17],[18],[19]

To evaluate and compare the value of demand side flexibility from different heating devices requires estimating the impact on power systems. Existing power system modelling often oversimplifies representation of flexibility constraints. When co-optimizing the domestic heating operation and dispatchable resources in the power system, Franken et al [20] assumed 12-hour load shifting capacity for heat pumps. While the majority of studies on system impact of HHPs do not explicitly account for building thermal inertia of dwellings, which neglects both HHPs' and MHPs' ability to provide load shifting with this inertia [21], [22], [23], [24], [25].

Additionally, the available demand response depends on the flexibility activation method used (i.e. incentive design and operation scheduling). To test and explore novel mechanisms suitable for a low-carbon power system context, the model used to represent domestic heating flexibility should be capable of responding to different activation methods of flexibility. Similarly, government subsidy programmes for deployment of low-carbon heating technologies including MHPs and HHPs, for example, the UK's Boiler Upgrade Scheme, can benefit from a model that reflects the variation of building thermal properties and how these impact the flexibility potential of the dwellings once equipped with MHPs or HHPs.

The dominant modeling approach for evaluating domestic heating flexibility are 'white-box' models (e.g. EnergyPlus) which model building thermal properties based on physical components. They require extensive building structure information and calibration, and cannot accurately represent short-term thermal dynamics with the duration of demand response events [26], [27], [28]. While 'black-box' models (e.g. Artificial Neural Networks) are capable of accurately capturing the temperature dynamics, this accuracy is achieved by using large numbers of parameters which then requires a high volume of training data to avoid overfitting. The resulting knowledge from such deep learning models is often non-transferable out of sample, i.e. when conditions including weather and flexibility activation methods change.

This study uses a framework based on the Grey-Box Lumped Capacitance modelling to represent domestic building thermal dynamics - drawing on real-world monitoring data from over 700 UK dwellings. This approach ensures accuracy by fitting parameters that minimizes the prediction error. It contains fewer parameters and requires significantly lower volumes of data compared to ANNs. The Grey-Box model is also linear and can be integrated into building operation models more easily, with the ability to alter weather and control assumptions to construct future scenarios.

2. Method

In this section, the modelling framework will be discussed in detail.

2.1. The Electrification of Heat dataset

The open-source data from the EoH (Electrification of Heat) project is used [29]. From 2020 to 2022, 750 UK dwellings with heat pumps were monitored in the project, 150 of which were HHPs, the rest being MHPs. The dataset includes monitoring data of indoor temperature, external temperature, heat output from the heating device, flow temperature, and the postcode of the dwellings which will be used to look up weather data. The dataset also provides a sufficient monitoring frequency for this model with a temporal resolution of 30 minutes. The dataset is cleansed in this study by filtering out empty data points and resampling from 2-minute to 30-minute resolution. The winter monitoring period (from December to February) is selected for training and testing the dataset. For each dwelling, 10 winter days with heat output are randomly selected for training and 5 for testing to fit the grey-box model, to avoid selection bias, and expose the model to multiple occupancy and weather patterns within a reasonable training time. After selection, 683 dwelling datasets contain sufficient data for the training and testing requirements.

2.2. The grey-box lumped-capacitance model

The grey-box lumped-capacitance model simplifies the building thermal structure into layers of thermal resistances and capacitances. It provides good estimation of short-term building thermal dynamics, at around 0.3-0.6K temperature prediction RMSE as by Hollick et al. [30] and Sperber et al.[31]. Bacher and Madsen [32] provide a wide range of grey-box models to represent the thermal dynamics of various types of buildings. Considering the number of dwellings to fit and the time constraint for this study, a model based on Hollick et al [30] is used.

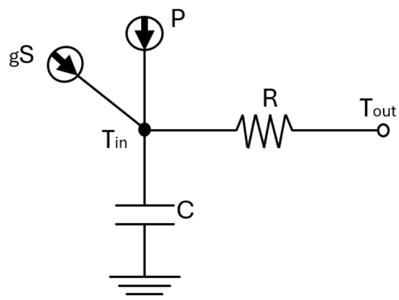

Figure 1 The grey-box lumped-capacitance model

As in Figure 1, the selected model consists of one thermal resistance R, one thermal capacitance C, a solar gain term gS, where S represents the solar irradiance, g represents the equivalent aperture of solar gain in the dwelling. P stands for the internal heat gain, which in this study consists entirely of the heating output. T_{out}, T_{in} are relatively the external and indoor air temperature. The thermal dynamic of this model is formulated as:

$$C\frac{dT_{in}(t)}{dt} = \frac{T_{out}(t) - T_{in}(t)}{R} + P(t) + gS(t) \quad (1)$$

, where the $T_{out}, T_{in}, P(t), S(t)$ are input variables available from the data, while C_1, R_1, g are the model parameters to be fitted for each dwelling.

The error function is calculated as the RMSE of the predicted indoor air temperature T_{in}^* generated using equation (1) against measured indoor air temperature T_{in}, as formulated in (2). It is the same case with the validation error, only calculated on the validation dataset.

$$Training\ Error = \sqrt{\sum_{t \in \tau_{training}} \frac{\left(T_{in}^{*}(t) - T_{in}(t)\right)^2}{n_{training}}} \tag{2}$$

2.3. Optimization of residential heating based on time-of-use tariff

The thermal dynamics captured by the above are used to construct an optimization problem for controlling domestic flexible demand regarding the given electricity tariff. In this model, smart control is assumed to optimize the fuel cost of the dwelling by scheduling HHP. For simplicity, tariffs are updated daily, and the control algorithm is assumed to have perfect next-day weather foresight to provide an upper-bound estimation of demand response.

The optimization problem for a single dwelling control with HHP is stated as follows:

$$\min_{P^e(t),P^g(t)} \sum_{t \in \tau} P^e(t)\pi^e(t) + P^g(t)\pi^g \tag{3}$$

$subject\ to$:

$$T_{(t)}^{lower} \leq T_{(t)}^{in} \leq T_{(t)}^{upper} \tag{4}$$

$$0 \leq P^g(t) \tag{5}$$

$$0 \leq P^g(t) \leq P_{up}^{g} \tag{6}$$

$$0 \leq P^e(t) \leq P_{up}^{e} \tag{7}$$

$$T^{in}(t+1) + \left(\frac{\Delta t}{RC} - 1\right)T^{in}(t) - \frac{\Delta t}{C}(Q^{heat} + Q^{solar}) - \frac{\Delta t}{RC}T^{out}(t) = 0 \tag{8}$$

$$Q^{heat}(t) = COP\ P^e(t) + \eta^g P^g(t) \tag{9}$$

, where the HHP is optimally scheduled to minimize the fuel cost[1].

The Octopus Cosy time-of-use tariff is used to incentivise peak shedding during evening peak hours from 16:00 to 19:00, as in Figure 2.

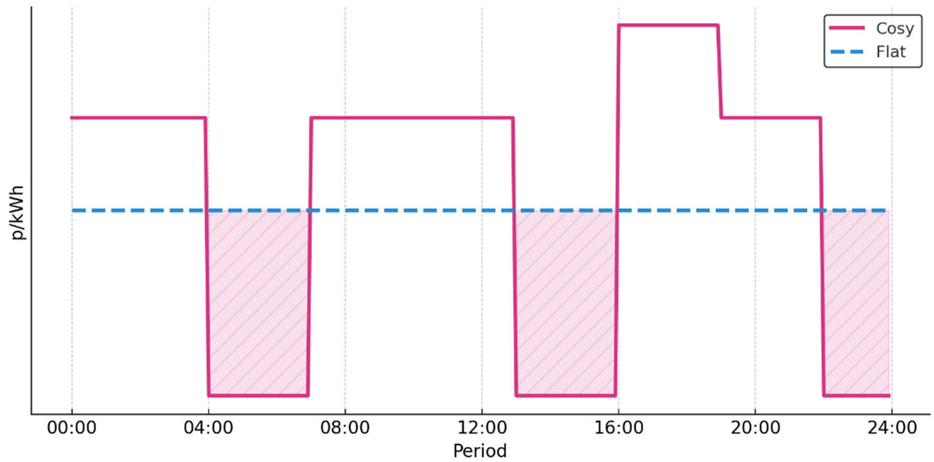

Figure 2 Octopus Cosy Tariff (Source: Octopus Cosy Website) [33]

[1] Hot water consumption and smart EV charging are yet to be added to the model

The output from this optimization model is the electricity and gas consumption curve during the test period. This is then used to calculate the demand response for each dwelling by subtracting the demand curve under a flat electricity price from the result under the time-of-use tariff. A five-day period of coldest days in February 2022 in EH33 Edinburgh is used for all dwellings to simulate a typical mild winter day, and another extreme weather scenario is made by subtracting 5 °C from the original mild weather profile. This provides a five-day period

3. Results and Discussion

In this section, the results of the above analysis are presented, including the resulting parameters fitted using the grey-box model and the energy consumption profile generated by the building heating optimization model.

3.1. Grey-box model fitting

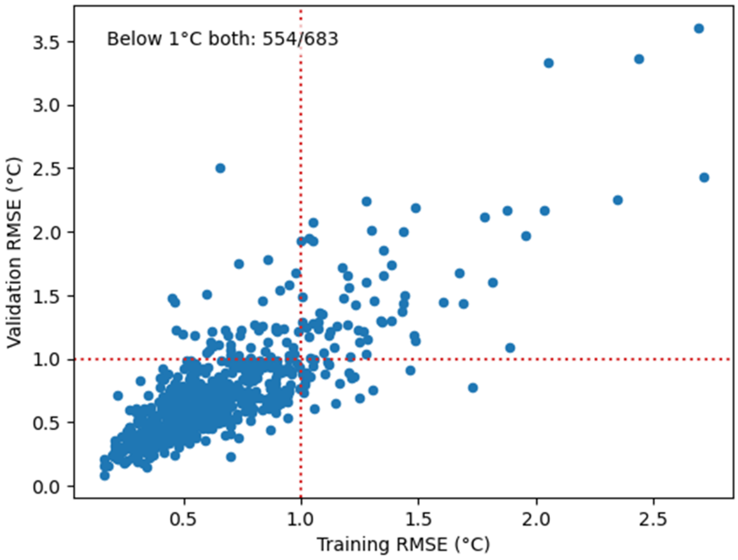

Figure 3 Training and validation error for dwellings in the dataset

Figure 3 shows the training and validation errors for 683 dwellings, which are positively correlated. Since the validation error does not rise as the training error decreases, there is no indication of overfitting. This study has selected a simple topology (the structure of the thermal resistance and capacitance network) of the grey-box model. To capture more accurate thermal characteristics of the dwellings, it is required to test and compare the performance of different topologies on each dwelling in future studies. In this analysis, it is inferred that the dwellings with less than 1 °C training and validation errors can be effectively represented by the proposed model, while the others are filtered out. This error margin can be explained by the fact that the dataset does not contain occupancy factors including window opening, alternative heat sources, and heat gains from other appliances. These factors will be assumed in the next section, where the thermal model is used for estimating the heat consumption in dwellings. In future developments, the assumptions will be improved for better realism. 508 dwellings remain after the above filtering. This shows that the topology selected for this study can only represent a portion of the dwellings in the dataset. In future studies, a variety of model topologies will be tested and compared for each dwelling.

The marginal and joint distribution of the thermal resistance and capacitance for the dwellings is shown in Figure 4. The 95% confidence interval of the thermal resistance is $(2 \times 10^{-3}, 3.3 \times 10^{-2})\ K/W$, which gives a range of heat transfer coefficients (HTC) of $(30\ , 500) W/K$, representing a wide range of dwellings from small, well-insulated flats to large, poorly-insulated houses. The 95% confidence interval of the thermal resistance also covers a wide range of $(8.6 \times 10^{6}, 2.5 \times 10^{8})\ J/K$. The outliers are excluded from the next step of the analysis. Another important metric is the thermal time constant, which indicates the speed of internal temperature exponential decay during a cool-down event without any heat gain into the building envelope:

$$\tau = RC \tag{10}$$

The distribution of the thermal time constant across dwellings is presented in Figure , where the empirical distribution fits well with a Log-normal distribution, with the mean at approximately 70 hours.

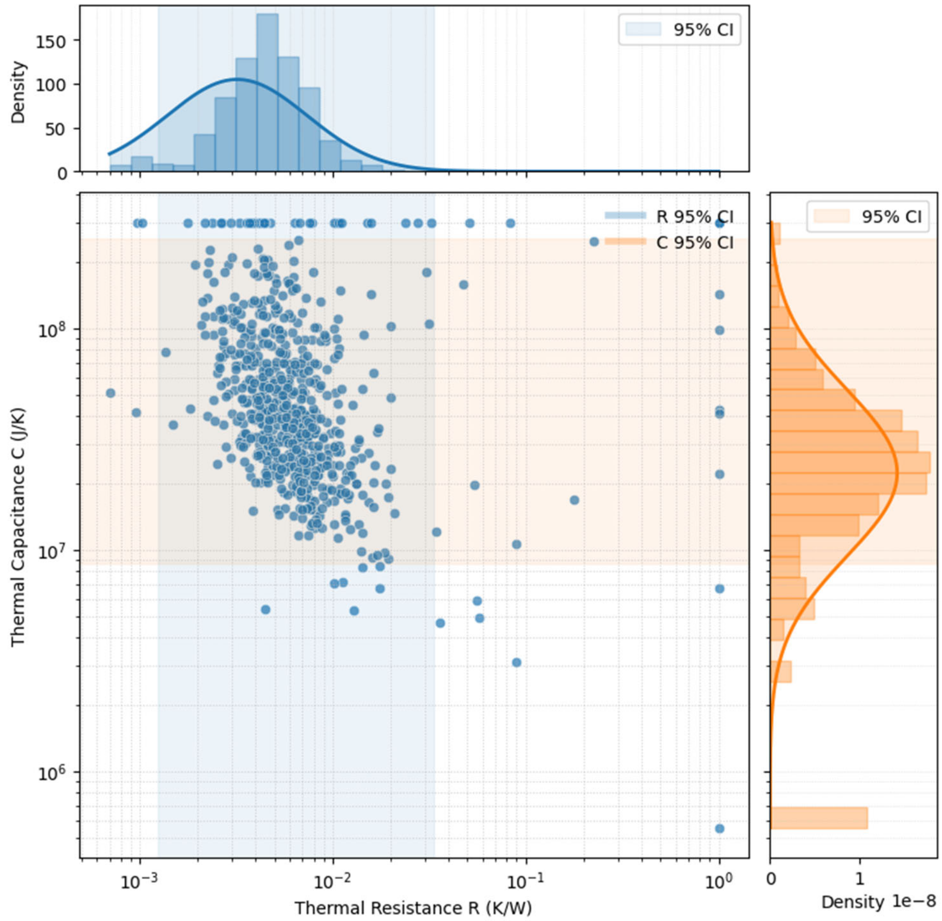

Figure 4 Distribution of thermal resistance and capacitance

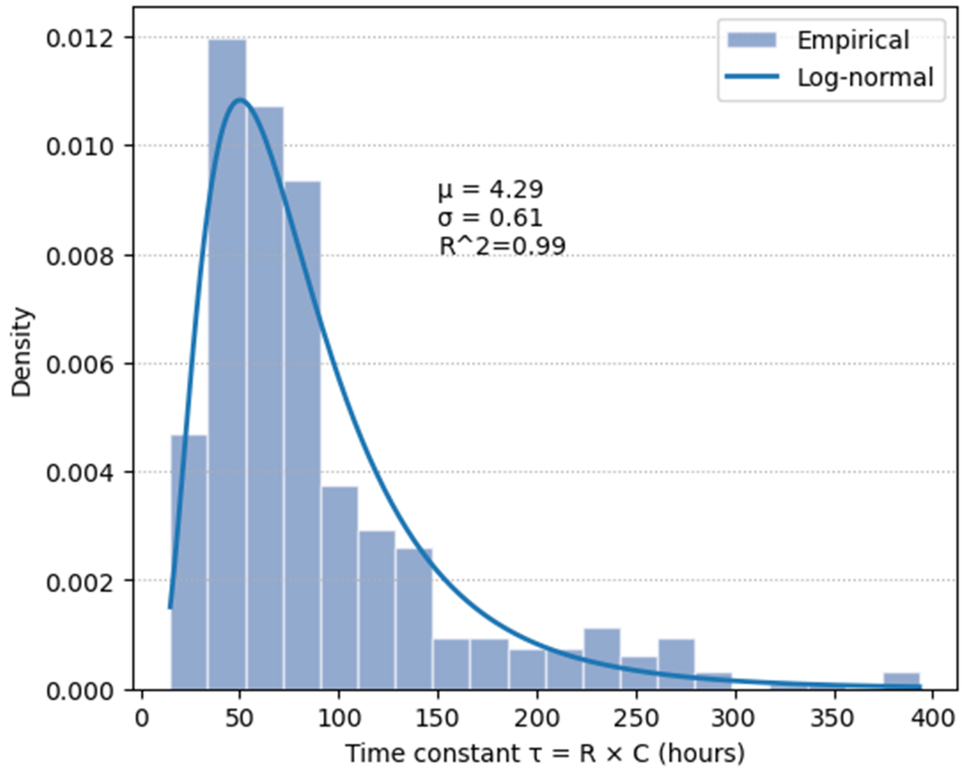

Figure 5 Distribution of building thermal time constant

3.2. Cost-optimal simulation of flexible heating

The parameters of the resulting 508 dwellings are put into the building heating optimization to simulate the heating consumption of these dwellings while optimally controlled to minimize fuel cost given a time-of-use tariff structure.

3.2.1. Peak time demand response by HHPs

The peak time demand response is calculated by comparing the case where the Cosy time-of-use tariff is applied and a counterfactual where the electricity price is constant throughout the simulation period. In Figure 6, the demand response during a 3-hour period 16:00-19:00 on the coldest day under the extreme weather scenario is presented. Although on average, the MHPs have more than 75% excess heat pump capacity compared with HHPs, they only provide around 30% more load reduction during this period. The HHP demand response shows high concentration around high end of the distribution, which is bound by the physical capacity of the heat pump component. This shows HHPs' ability to provide significant load reduction capacity during peak demand times, even with a much smaller heat pump than conventional MHPs.

Figure 7 provides a closer examination of the peak time demand response potential's correlation with the building thermal parameters. There is no clear correlation observed with the effective solar gain aperture, and thermal constant. A subtle positive correlation is observed with the thermal capacitance, as the capacitances increase, the building envelopes have stronger ability to store heat.

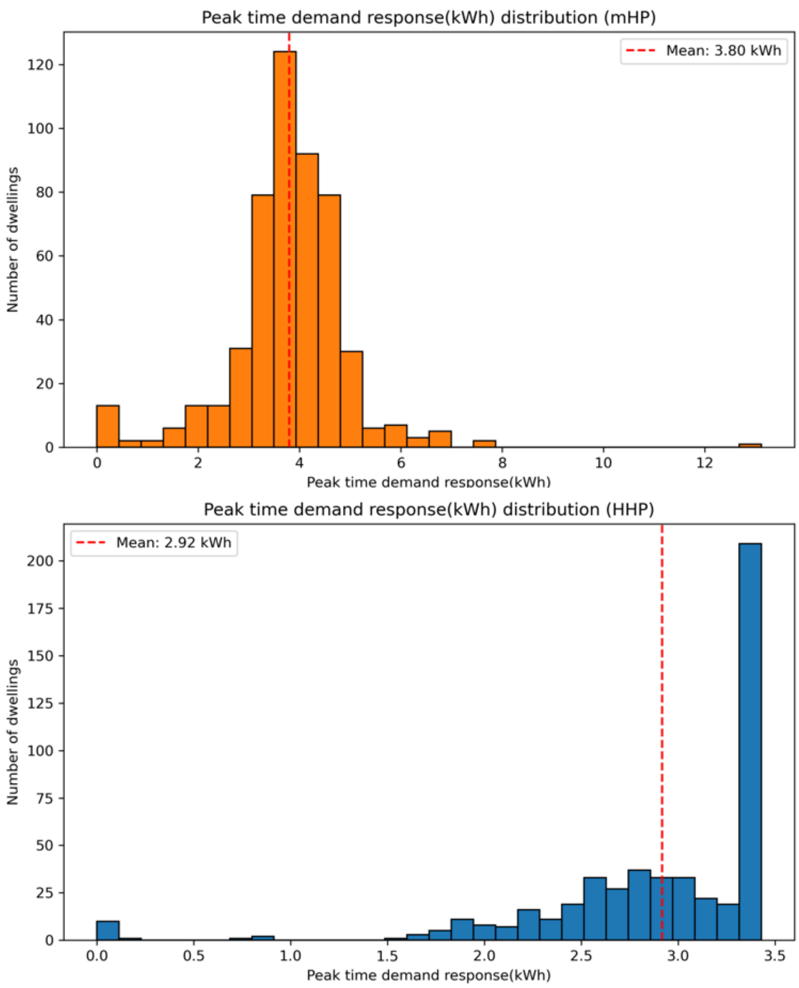

Figure 6 Peak time demand response by HHP and MHP during peak period of 3 hours

The peak reduction potential of both HHPs and MHPs is found to be significantly inversely proportional to the thermal resistance, which means it is also proportional the HTC. During peak demand period, the heat pump is used for maintaining temperature level, instead of giving rapid boost of temperature like boilers are capable of. This means that under the non-flexible case the heat pump output is equal to the instantaneous heat loss, which is proportional to the HTC, given constant indoor-outdoor temperature difference. There is also a pattern when the HTC increases and the heat pump component reaches capacity, the demand response potential is capped. In this case, the model has successfully captured the above patterns.

Although the demand response by HHPs is found to be less than that of MHPs, the contribution to the aggregated peak load from an HHP is smaller because the boiler has been able to undertake a portion of the peak load.

3.3. Electrification of space heating demand

As in Figure 8, an average of 86% of space heating demand is delivered with the 4kW heat pump component of HHP, with concentration at the higher end. This emphasizes HHPs' ability to electrify most of the heating demand even during low temperature periods. Figure 9 shows the correlation between electrification proportion and multiple building thermal parameters. There is a significantly positive correlation between thermal resistance and the electrification proportion. As the dwelling becomes better insulated, the peak load reduces, which requires less boiler heat in addition to the heat pump.

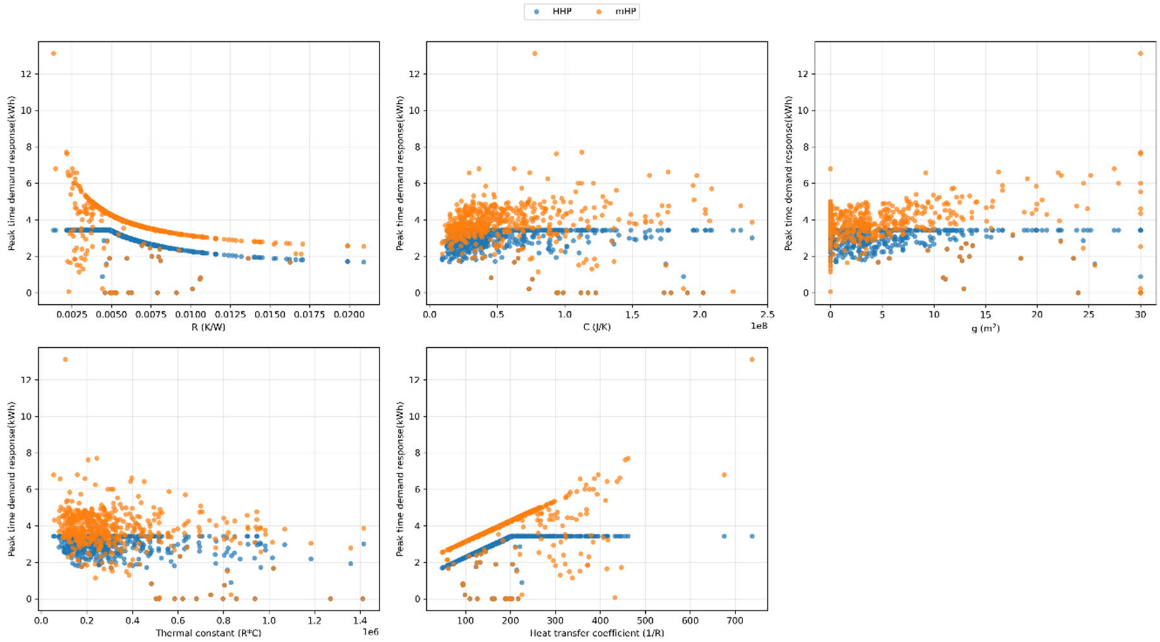

Figure 7 Correlation between the peak time demand response of MHPs and HHPs with building thermal properties

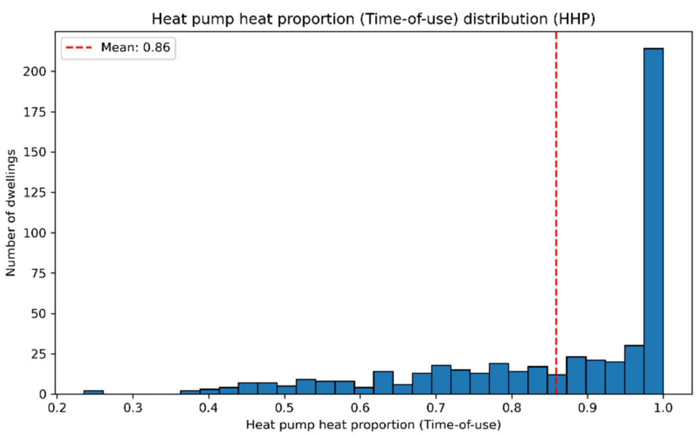

Figure 8 Proportion of heating delivered with electricity by HHPs (Extreme Weather Case)

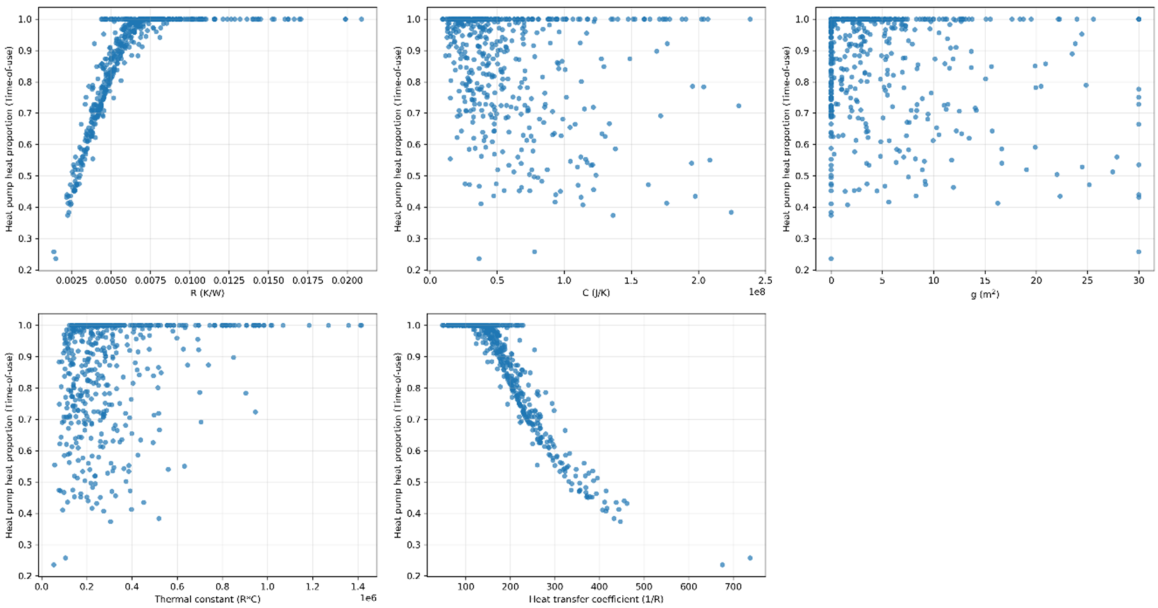

Figure 9 Correlation of electrification proportion and the building thermal parameters

4. Conclusion

This study provides a framework to extract empirical information from a large number of UK dwellings to investigate and compare how flexible HHP and MHP perform subject to various building thermal properties. It is found that HHPs can on average electrify 86% percent of space heating, provide 77% of MHP peak time demand response while only having half of the heat pump capacity. The electrification and flexibility potential is found to be most relevant to the thermal resistance (i.e. the reciprocal of the HTC), among all building thermal parameters.

This work provides increased granularity of domestic heating flexibility modelling, and can be further applied to power system modelling to evaluate the flexibility from dwellings with different thermal conditions.

As early-stage work, it has not considered several important components of the built environment, including different patterns of thermal comfort (which can be considered by altering the temperature setpoint curve), and other alternative technologies that provide flexibility, predominantly electric vehicles. The accuracy of the grey-box modelling should also be increased by fitting and comparing different model topologies for each dwelling. Last but not least, it is worth noting that although this work features reflecting the variation of heating flexibility among dwellings, it does not provide a representative portfolio of dwelling models for the UK building stock, which is limited by the scope of the available dataset.

It is also worth noting that although an individual HHP provides less demand response than an MHP, it contributes less to peak demand. From a low-voltage (LV) network perspective, this allows the limited capacity headroom to accommodate a greater number of HHPs than MHPs, potentially enabling higher levels of heat electrification and greater aggregate demand response potential—an aspect that will be examined in future work.

Nomenclature

$t \in \tau$ — discrete time step (half-hourly)
P^e — electrical input power of the heat pump [kW]
P^g — gas input power of the boiler [kW]
Q^{heat} — useful space heating output [kW]
Q^{solar} — solar heat gains [kW]
$\pi^e(t)$ — time-varying electricity tariff [£/kWh]
π^g — static gas price[£/kWh]
COP — coefficient of performance of the heat pump [–]
η^g — boiler efficiency [–]
R — lumped thermal resistance of dwelling [K/kW]
C — lumped thermal capacitance of dwelling [kWh/K]
Δt — simulation time step [h]
$T^{in}(t)$ — indoor air temperature [°C]
$T^{out}(t)$ — external air temperature [°C]
$T^{lower}(t), T^{upper}(t)$ — time-variant comfort bounds on indoor temperature [°C]

Acknowledgements

This research was made possible by support from the EPSRC Centre for Doctoral Training in Energy Resilience and the Built Environment (ERBE), grant number EP/S021671/1 and with in-kind and financial support from Worcester Bosch. Special thanks to Dr Daniel Scamman, Dr Frances Hollick and Dr Jenny Crawley for support in administration and conceptualization.

References

[1] Department for Energy Security and Net Zero, 'Heat Pump Investment Roadmap', 2023.
[2] Climate Change Committee, *The Sixth Carbon Budget*. 2020.
[3] D. Pudjianto *et al.*, 'Smart control for minimizing distribution network reinforcement cost due to electrification', *Energy Policy*, vol. 52, pp. 76–84, Jan. 2013, doi: 10.1016/j.enpol.2012.05.021.
[4] T. Boßmann and I. Staffell, 'The shape of future electricity demand: Exploring load curves in 2050s Germany and Britain', *Energy*, vol. 90, pp. 1317–1333, Oct. 2015, doi: 10.1016/j.energy.2015.06.082.
[5] S. D. Watson, J. Crawley, K. J. Lomas, and R. A. Buswell, 'Predicting future GB heat pump electricity demand', *Energy Build.*, vol. 286, p. 112917, May 2023, doi: 10.1016/j.enbuild.2023.112917.
[6] N. Lamb and D. Elmes, 'Increasing heat pump adoption: analysing multiple perspectives on preparing homes for heat pumps in the UK', *Carbon Neutrality*, vol. 3, no. 1, p. 10, Dec. 2024, doi: 10.1007/s43979-024-00084-w.
[7] Climate Change Committee, 'Progress in reducing emissions - 2025 report to Parliament', Accessed: Aug. 22, 2025. [Online]. Available: https://www.theccc.org.uk/publication/progress-in-reducing-emissions-2025-report-to-parliament/
[8] Climate Change Committee, 'A Net Zero workforce', May 2023, [Online]. Available: https://www.theccc.org.uk/wp-content/uploads/2023/05/CCC-A-Net-Zero-Workforce-Web.pdf?utm_source=chatgpt.com
[9] J. Speirs, P. Balcombe, E. Johnson, J. Martin, N. Brandon, and A. Hawkes, 'A greener gas grid: What are the options', *Energy Policy*, vol. 118, pp. 291–297, July 2018, doi: 10.1016/j.enpol.2018.03.069.
[10] M. Beccali, M. Bonomolo, F. Martorana, P. Catrini, and A. Buscemi, 'Electrical hybrid heat pumps assisted by natural gas boilers: a review', *Appl. Energy*, vol. 322, p. 119466, Sept. 2022, doi: 10.1016/j.apenergy.2022.119466.
[11] S. Heinen, D. Burke, and M. O'Malley, 'Electricity, gas, heat integration via residential hybrid heating technologies – An investment model assessment', *Energy*, vol. 109, pp. 906–919, Aug. 2016, doi: 10.1016/j.energy.2016.04.126.
[12] G. Bennett, S. Watson, G. Wilson, and T. Oreszczyn, 'Domestic heating with compact combination hybrids (gas boiler and heat pump): A simple English stock model of different heating system scenarios', *Build. Serv. Eng. Res. Technol.*, vol. 43, no. 2, pp. 143–159, Mar. 2022, doi: 10.1177/01436244211040449.
[13] Department for Energy Security and Net Zero,'Clean Power 2030 Action Plan: A new era of clean

electricity', 2030.
[14] J. Love *et al.*, 'The addition of heat pump electricity load profiles to GB electricity demand: Evidence from a heat pump field trial', *Appl. Energy*, vol. 204, pp. 332–342, Oct. 2017, doi: 10.1016/j.apenergy.2017.07.026.
[15] M. Pullinger *et al.*, 'Capturing variation in daily energy demand profiles over time with cluster analysis in British homes (September 2019 – August 2022)', *Appl. Energy*, vol. 360, p. 122683, Apr. 2024, doi: 10.1016/j.apenergy.2024.122683.
[16] H. Li, Z. Wang, T. Hong, and M. A. Piette, 'Energy flexibility of residential buildings: A systematic review of characterization and quantification methods and applications', *Adv. Appl. Energy*, vol. 3, p. 100054, Aug. 2021, doi: 10.1016/j.adapen.2021.100054.
[17] PassivSystems Ltd,'Freedom Project Final Report', October 2018, https://commercial.nationalgrid.co.uk/downloads/12221/freedom-project-final-report.pdf
[18] J. Crawley, G. Moore, S. Higginson, C. Elwell, and N. Eyre, 'The Role of Domestic Heat Pumps in Providing Flexibility to the UK Electricity System', *Energies*, vol. 17, no. 12, p. 2995, June 2024, doi: 10.3390/en17122995.
[19] M. Qadrdan, 'Overview of flexibility services in the GB power system'.
[20] L. Franken *et al.*, 'Power system benefits of simultaneous domestic transport and heating demand flexibility in Great Britain's energy transition', *Appl. Energy*, vol. 377, p. 124522, Jan. 2025, doi: 10.1016/j.apenergy.2024.124522.
[21] L. Jin, X. Li, S. De Lange, H. Slootweg, and N. G. Paterakis, 'Response Allocation of Domestic Hybrid Heat Pumps Flexibility for Congestion Management', in *2024 IEEE PES Innovative Smart Grid Technologies Europe (ISGT EUROPE)*, Dubrovnik, Croatia: IEEE, Oct. 2024, pp. 1–5. doi: 10.1109/ISGTEUROPE62998.2024.10863630.
[22] N. Loomans and F. Alkemade, 'Exploring trade-offs: A decision-support tool for local energy system planning', *Appl. Energy*, vol. 369, p. 123527, Sept. 2024, doi: 10.1016/j.apenergy.2024.123527.
[23] F. Wüllhorst, S. Schwarz, N. Fuchs, L. Maier, A. Monti, and D. Müller, 'Impact of hybrid heat pump shares and building envelope retrofit rates on load penetration in German low-voltage grids', *Appl. Energy*, vol. 388, p. 125530, June 2025, doi: 10.1016/j.apenergy.2025.125530.
[24] E. Zeyen, 'Mitigating heat demand peaks in buildings in a highly renewable European energy system', 2021.
[25] X. Zhang, G. Strbac, N. Shah, F. Teng, and D. Pudjianto, 'Whole-System Assessment of the Benefits of Integrated Electricity and Heat System', *IEEE Trans. Smart Grid*, vol. 10, no. 1, Art. no. 1, Jan. 2019, doi: 10.1109/TSG.2018.2871559.
[26] M. Wetter, K. Benne, H. Tummescheit, and C. Winther, 'Spawn: coupling Modelica Buildings Library and EnergyPlus to enable new energy system and control applications', *J. Build. Perform. Simul.*, vol. 17, no. 2, pp. 274–292, Mar. 2024, doi: 10.1080/19401493.2023.2266414.
[27] Z. Chen *et al.*, 'An Analysis of the Hybrid Internal Mass Modeling Approach in EnergyPlus'.
[28] R. Li, 'Modelling of possible Energy Flexibility in Single Buildings and Building Clusters'.
[29] Heating & Hotwater Industry Council, 'Hybrid Heat Pumps: A Flexible Route to Decarbonise Heat', 2022. [Online]. Available: https://www.hhic.org.uk/resources/9
[30] F. P. Hollick, V. Gori, and C. A. Elwell, 'Thermal performance of occupied homes: A dynamic grey-box method accounting for solar gains', *Energy Build.*, vol. 208, p. 109669, Feb. 2020, doi: 10.1016/j.enbuild.2019.109669.
[31] E. Sperber, U. Frey, and V. Bertsch, 'Reduced-order models for assessing demand response with heat pumps – Insights from the German energy system', *Energy Build.*, vol. 223, p. 110144, Sept. 2020, doi: 10.1016/j.enbuild.2020.110144.
[32] P. Bacher and H. Madsen, 'Identifying suitable models for the heat dynamics of buildings', *Energy Build.*, vol. 43, no. 7, pp. 1511–1522, July 2011, doi: 10.1016/j.enbuild.2011.02.005.
[33] Octopus Energy, 'Cosy Octopus The smart electricity tariff designed to keep homes toasty'. [Online]. Available: https://octopus.energy/smart/cosy-octopus/